

Cerebellar asymmetry and its relation to cerebral asymmetry estimated by intrinsic functional connectivity

Danhong Wang, Randy L. Buckner and Hesheng Liu

J Neurophysiol 109:46-57, 2013. First published 17 October 2012; doi:10.1152/jn.00598.2012

You might find this additional info useful...

This article cites 64 articles, 30 of which can be accessed free at:

</content/109/1/46.full.html#ref-list-1>

This article has been cited by 1 other HighWire hosted articles

Neurobiological basis of head motion in brain imaging

Ling-Li Zeng, Danhong Wang, Michael D. Fox, Mert Sabuncu, Dewen Hu, Manling Ge, Randy L. Buckner and Hesheng Liu

PNAS, April 22, 2014; 111 (16): 6058-6062.

[\[Abstract\]](#) [\[Full Text\]](#) [\[PDF\]](#)

Updated information and services including high resolution figures, can be found at:

</content/109/1/46.full.html>

Additional material and information about *Journal of Neurophysiology* can be found at:

<http://www.the-aps.org/publications/jn>

This information is current as of June 20, 2014.

Cerebellar asymmetry and its relation to cerebral asymmetry estimated by intrinsic functional connectivity

Danhong Wang,^{1,2} Randy L. Buckner,^{1,2,3,4} and Hesheng Liu¹

¹Athinoula A. Martinos Center for Biomedical Imaging, Department of Radiology, Massachusetts General Hospital, Charlestown, Massachusetts; ²Department of Psychiatry, Massachusetts General Hospital, Boston, Massachusetts;

³Department of Psychology and Center for Brain Science, Harvard University, Cambridge, Massachusetts; ⁴Howard Hughes Medical Institute, Cambridge, Massachusetts

Submitted 12 July 2012; accepted in final form 16 October 2012

Wang D, Buckner RL, Liu H. Cerebellar asymmetry and its relation to cerebral asymmetry estimated by intrinsic functional connectivity. *J Neurophysiol* 109: 46–57, 2013. First published October 17, 2012; doi:10.1152/jn.00598.2012.—Asymmetry of the human cerebellum was investigated using intrinsic functional connectivity. Regions of functional asymmetry within the cerebellum were identified during resting-state functional MRI ($n = 500$ subjects) and replicated in an independent cohort ($n = 500$ subjects). The most strongly right lateralized cerebellar regions fell within the posterior lobe, including crus I and crus II, in regions estimated to link to the cerebral association cortex. The most strongly left lateralized cerebellar regions were located in lobules VI and VIII in regions linked to distinct cerebral association networks. Comparison of cerebellar asymmetry with independently estimated cerebral asymmetry revealed that the lateralized regions of the cerebellum belong to the same networks that are strongly lateralized in the cerebrum. The degree of functional asymmetry of the cerebellum across individuals was significantly correlated with cerebral asymmetry and varied with handedness. In addition, cerebellar asymmetry estimated at rest predicted cerebral lateralization during an active language task. These results demonstrate that functional lateralization is likely a unitary feature of large-scale cerebrocerebellar networks, consistent with the hypothesis that the cerebellum possesses a roughly homotopic map of the cerebral cortex including the prominent asymmetries of the association cortex.

lateralization; cerebellum; functional magnetic resonance imaging; functional connectivity

WHILE FUNCTIONAL ASYMMETRIES of the cerebral cortex and other brain structures have been explored extensively (Gazzaniga 2000; Geschwind and Galaburda 1985; Milner et al. 1997), asymmetry within the cerebellum is poorly understood, especially for regions of the cerebellum linked to the association cortex. The cerebellum is connected to the cerebral cortex through polysynaptic circuits that are preferentially contralateral (Evarts and Thach 1969; Kemp and Powell 1971; Schmahmann and Pandya 1997; Strick 1985) and involve multiple closed-loop connections such that a region of the cerebral cortex sends and receives projections from the same region of the cerebellum (Kelly and Strick 2003; Strick et al. 2009). Neuroimaging studies of asymmetric cerebral functions have often found similarly asymmetric (but flipped) functional responses in the cerebellum (for a recent meta-analysis, see

Stoodley and Schmahmann 2009). For example, in most people, language processing activates the left inferior frontal gyrus and superior temporal lobe as well as the right cerebellum, including crus I/II and lobule VI. In contrast, spatial processing often involves the right angular gyrus, supramarginal gyrus, insula, and left lobule VI of the cerebellum. A reasonable hypothesis based on these anatomic and neuroimaging observations is that functional asymmetries within the cerebellum will organize as anatomically flipped versions of functional asymmetries present in the cerebral cortex. The primary goal of the present study was to explore the hypothesis that functional asymmetries in the cerebellum parallel functional asymmetries present in the cerebral cortex.

Multiple lines of evidence suggest that cerebellar asymmetry may covary with the cerebral asymmetry. For example, cerebellar lateralization switches in parallel with cerebral language lateralization in poststroke patients (Connor et al. 2006), and individuals with congenital focal lesions in the left cerebral hemisphere show a reorganized language network involving the left cerebellum (Lidzba et al. 2008). Cerebellar volume asymmetry follows the same laterality pattern in the cerebral cortex and is associated with handedness (Snyder et al. 1995). These collective findings reinforce the expectation that cerebral and cerebellar asymmetries track one another, including for the association cortex.

There is a second important reason to explore functional asymmetry of the cerebellum. A major challenge facing the investigation of functional asymmetry is the pronounced anatomic asymmetries in the human brain (for a review, see Toga and Thompson 2003). At the macroscopic level, the cerebral cortex exhibits asymmetry in overall morphology (Geschwind and Levitsky 1968; Witelson and Pallie 1973), cortical folding pattern (Hill et al. 2010), surface area (White et al. 1994), and gray matter thickness (Luders et al. 2006). Microscopically, hemispheric asymmetry has been observed in various cerebral areas in terms of the cytoarchitecture (Amunts et al. 1999, 2003) and the organization of the microcircuitry (Galuske et al. 2000). Anatomic asymmetry of the cerebral cortex causes significant difficulties when functional measures are contrasted between homotopic regions in the two hemispheres (Anderson et al. 2011; Liu et al. 2009). One cannot deconfound whether there is a true functional asymmetry or an apparent functional difference secondary to anatomic misalignment. Our own work on cerebral asymmetries contain this confound (Liu et al. 2009). Although surface registration based on anatomic landmarks (Fischl et al. 1999a; Van Essen et al. 2011) partially

Address for reprint requests and other correspondence: H. Liu, Athinoula A. Martinos Center for Biomedical Imaging, Massachusetts General Hospital, 149 13th St., Suite 2301, Charlestown, MA 02129 (e-mail: Hesheng@nmr.mgh.harvard.edu).

addresses the problem, functional asymmetry could still be confounded when cytoarchitecture does not respect macroscopic anatomical landmarks. Examining the functional asymmetry of the cerebellum is thus also of interest because it provides an independent means to explore the functional lateralization of the human brain. The cerebellum has a generally symmetric overall morphology and a much simpler cytoarchitecture than the cerebral cortex (Ito 1984). If the cerebellum possesses a roughly homotopic map of the cerebral cortex, including the asymmetric association cortex, then examination of its functional organization provides another way to understand the functional asymmetry of the cerebral cortex.

In this study, we sought to characterize the lateralized regions in the human cerebellum and investigate the relation between cerebellar asymmetry and cerebral asymmetry. We developed a novel method based on intrinsic functional connectivity measured by resting-state functional MRI (fMRI) (Biswal et al. 1995) to quantify the functional laterality of the cerebral cortex, cerebellum, and cerebrocerebellar coupling. This method allowed a map of cerebellar asymmetries to be constructed in an unbiased manner and directly compared with an independently estimated map of cerebral asymmetries. We found that lateralization of the cerebellum tracks the lateralization in the cerebral cortex both in terms of which networks are lateralized and the degree to which laterality varies between subjects. These results tentatively suggest that asymmetry is a unitary feature of large-scale cerebrocerebellar networks.

MATERIALS AND METHODS

Participants. Data were acquired as part of the Brain Genomics Superstruct Project. Participants were enrolled by multiple local laboratories, all acquiring similar data on four matched 3T MRI scanners (one at Harvard and three at the Massachusetts General Hospital). All participants were native English speakers and had normal or corrected-to-normal vision. Participants were excluded with a history of neurological or psychiatric illness. Data from 1,000 participants were selected from a pool of 1,480 participants using the following criteria: 12-channel head coil (140 participants excluded), age between 18 and 35 yr (125 participants excluded), and fMRI slice-based temporal signal-to-noise ratio > 100 [84 participants excluded (see Van Dijk et al. 2012)]; 1,131 subjects remained after quality control, and the first 1,000 subjects according to the enrollment dates were included (mean age: 21.3 yr, 42.7% male and 57.3% female, 90.9% right handed and 9.1% left handed). The 1,000 subjects were divided into 2 independent samples ($n = 500$ samples each, labeled as “discovery” and “replication” samples) that were matched for age, sex, and MRI scanner. Fifty-five subjects also participated in a task-based fMRI semantic classification paradigm; 49 subjects were from the 1,000 participants described above. Finally, all available left-handed individuals that met the inclusion criteria ($n = 52$ participants) were matched to 52 right-handed individuals for the exploration of handedness effects (see Table 1 for the matching criteria and participant demographics). All participants provided written informed consent in accordance with guidelines set by Institutional Review Boards of Harvard University or Partners Healthcare. Portions of these data have been previously reported (Yeo et al. 2011; Buckner et al. 2011; Choi et al. 2012; Van Dijk et al. 2012).

MRI data acquisition. Each participant performed one or two resting-state (eyes open) fMRI runs (6 min and 12 s per run, mean: 1.7 runs). All data were collected on matched 3T Tim Trio scanners (Siemens, Erlangen, Germany) using a 12-channel phased-array head coil. Images were acquired using a gradient-echo echo-planar pulse sequence sensitive to blood oxygenation level-dependent (BOLD) contrast [repetition time (TR) = 3,000 ms, echo time (TE) = 30 ms,

Table 1. Demographic and imaging characteristics

Measure	Left-Handed Group		Right-Handed Group		<i>P</i> Value
	Mean	SD	Mean	SD	
Age, yr	19.9	1.9	19.9	1.7	0.90
Education, yr	13.8	1.7	13.8	1.5	0.67
Handedness	-16.7	4.8	16.6	4.7	
Runs	2	0	2	0	
Displacement, mm	0.05	0.02	0.05	0.02	0.92
Signal-to-noise ratio	183.4	36.4	183.4	34.0	0.98

Note that the two groups were also matched for scanner, console, ethnicity (5 Hispanic subjects/group), and investigator acquiring the data.

flip angle = 85°, 3 × 3 × 3-mm voxels, field of view (FOV) = 216; 47 slices collected with interleaved acquisition with no gap between slices]. Whole brain coverage included the entire cerebellum. Slices were aligned to the anterior commissure-posterior commissure plane using an automated alignment procedure to ensure consistency across subjects (van der Kouwe et al. 2008). Structural data used a high-resolution multiecho T1-weighted magnetization-prepared gradient-echo image (TR = 2200 ms, TI = 1100 ms, TE = 1.54 ms for *image 1* to 7.01 ms for *image 4*, flip angle = 7°, 1.2 × 1.2 × 1.2-mm voxels, and FOV = 230). Subjects were instructed to stay awake, keep their eyes open, and minimize head movement; no other task instruction was provided.

fMRI and structural MRI data processing. Resting-state fMRI data were processed using previously described procedures (Buckner et al. 2011; Van Dijk et al. 2010; Vincent et al. 2006; Yeo et al. 2011), which were adapted from Biswal et al. (1995) and Fox et al. (2005). The following steps were performed: 1) slice timing correction (SPM2, Wellcome Department of Cognitive Neurology, London, UK); 2) rigid body correction for head motion with the FSL package (Jenkinson et al. 2002; Smith et al. 2004); 3) normalization for global mean signal intensity across runs; and 4) low-pass temporal filtering, head motion regression, whole brain signal regression, and ventricular and white matter signal regression.

Structural data were processed using the FreeSurfer (version 4.5.0) software package, as previously described by Yeo et al. (2011). The version and processing environment were held constant for analysis of the full data sample. Surface mesh representations of the cortex from individual structural images were reconstructed and registered to a common spherical coordinate system (Dale et al. 1999; Fischl et al. 1999a, 1999b, 2001; Segonne et al. 2004, 2007). Structural and functional images were aligned using boundary-based registration (Greve and Fischl 2009) within the FsFast software package (<http://surfer.nmr.mgh.harvard.edu/fswiki/FsFast>). Resting-state BOLD fMRI data were then aligned to the common spherical coordinate system via sampling from the middle of the cortical ribbon in a single interpolation step (for details, see Yeo et al. 2011).

In this study, a symmetric surface template of the cerebral cortex was constructed. The symmetric surface template was downsampled to 642 vertices in each hemisphere. fMRI data of each individual were then registered to this template, thus allowing a direct comparison between anatomically homologous regions between the two hemispheres.

Hybrid surface- and volume-based alignment. The cerebral signal and cerebellar signal were aligned to the templates using a hybrid surface- and volume-based approach (Buckner et al. 2011). The cerebral cortex was modeled as a surface as previously described by Yeo et al. (2011), and the cerebellum was aligned using nonlinear volumetric registration as previously described by Buckner et al. (2011). The volumetric registration algorithm was proceeded by jointly deforming the structural volume to a probabilistic template and classifying each native brain voxel into one of multiple brain structures, including left and right cerebellar gray and white matter (Fischl

et al. 2002, 2004a, 2004b). A nonlinear deformation was used to reduce intersubject anatomic variability (Buckner et al. 2011). The resulting volumetric fMRI data were smoothed with a 6-mm full-width half-maximum smoothing kernel constrained by the cerebellum mask defined using the FreeSurfer template (Fischl et al. 2002, 2004a, 2004b). All cerebellar analyses were performed in FreeSurfer nonlinear volumetric space.

Visual inspection of the registered data suggested that accurate representations of the cerebellum and cortical surface were obtained for each participant and that structural and functional image registrations were successful. In addition, the volumetric registration was verified to ensure that the cerebellum was successfully aligned between subjects.

Regressing neighboring cerebral signal from the cerebellum. The close physical proximity of the anterior cerebellum to the visual cerebral cortex results in a blurring of the fMRI signal across the cerebellar–cerebral boundary. The signal arising from the cerebral cortex adjacent to the cerebellum was regressed from the cerebellar signal using masks of the left and right cerebral cortex within 6 and 7 mm, respectively, from the cerebellum. The spatial extent of the cerebellum was defined using the FreeSurfer template (Fischl et al. 2002, 2004a, 2004b). For each individual participant, the fMRI signal within the left and right cerebral cortex masks were averaged and regressed from the smoothed fMRI data within the cerebellum (Buckner et al. 2011). This regression procedure allows mapping of the full surface of the anterior lobe.

Region of interests defined in the cerebellum and cerebrum. We used a symmetric cortical surface template, which consists of 642 vertices on each hemisphere. Each one of these vertices was then taken as a region of interest (ROI). To determine the cerebellar ROIs, we uniformly sampled the left cerebellar hemisphere in the FreeSurfer nonlinear volumetric space into 275 cubic voxels (8 × 8 × 8 mm). These 275 ROIs were then registered to the right cerebellar hemisphere using a nonlinear transform (Andersson et al. 2007). The original ROI in the left hemisphere and its projection in the right hemisphere were treated as homologous ROIs. This procedure is imperfect owing to uncertainty of the exact appropriate left-right correspondence.

The hybrid surface- and volume-based alignment allowed us to perform region-based analyses between the cerebellum of a subject in FreeSurfer nonlinear volume space and the cerebrum of the same subject in FreeSurfer surface space. To evaluate functional connectivity, preprocessed resting fMRI time courses were extracted from surface ROIs in the cerebral cortex and volume ROIs in the cerebellum. Pearson's product-moment correlation was then computed between these ROIs. Fisher's r - to z -transformed correlations were computed for each subject.

The quantitative intrinsic laterality index. The intrinsic laterality index (iLI) was computed based on the asymmetric functional connectivity between homologous ROI pairs. The cerebral surface template consisted of 642 triangular vertices in each hemisphere, and the cerebellum consisted of 275 cubic ROIs in each hemisphere. We computed the functional correlation between all possible ROI pairs. There were 205,761 cerebral ROI pairs, 37,675 cerebellar ROI pairs, and 176,550 cerebrocerebellar ROI pairs in each hemisphere. Note that here each cerebrocerebellar ROI pair consist of an ROI on the cerebral surface and an ROI in the contralateral cerebellar volume.

The iLI was then computed based on the following relative correlation differences between two homologous ROI pairs according to Eq. 1:

$$iLI = \frac{P1 - P2}{P1 + P2} \quad (1)$$

where P1 is the functional correlation between an ROI pair within the right cerebellar cortex (Fig. 1A), an ROI pair between right cerebral cortex and left cerebellum (Fig. 1B), or a pair within the right cerebral

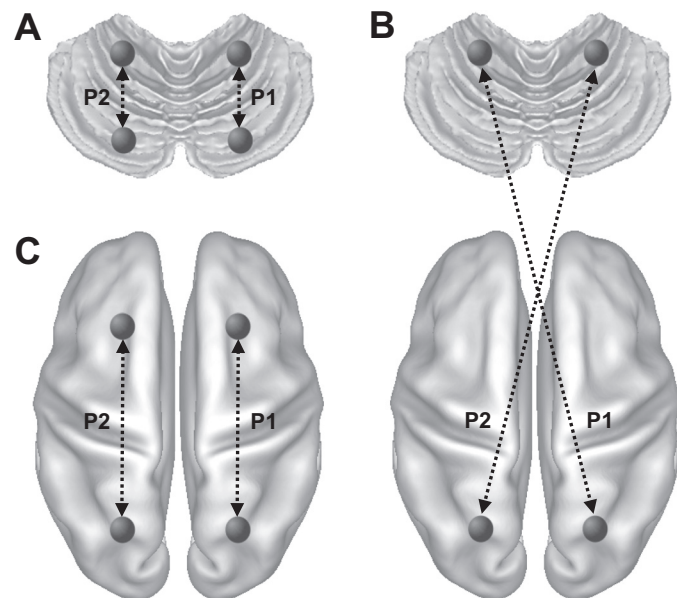


Fig. 1. Quantitative intrinsic laterality index (iLI). The iLI was computed for each region of interest (ROI) pair. The cerebral surface consisted of 642 ROIs in each hemisphere, and the cerebellum consisted of 275 cubic ROIs in each hemisphere. Functional correlations between all possible ROI pairs, including 37,675 × 2 cerebellar ROI pairs (A), 88,275 × 2 cerebrocerebellar ROI pairs (B), 205,761 × 2 cerebral ROI pairs (C), were computed. The iLI was then calculated based on the connectivity difference between homologous pairs according to Eq. 1 (see MATERIALS AND METHODS). P1 and P2 represent the connectivity of two homologous pairs.

cortex (Fig. 1C) and P2 is the correlation strength in the homologous pair. Therefore, iLI ranged from -1 to $+1$, with a positive value indicating right lateralization.

For each one of these pairwise correlations, we averaged the corresponding iLI values across the discovery data set of 500 individuals. The resulting mean iLIs were then sorted to determine those regions showing the strongest levels of lateralization. We selected the top 100 cerebral iLIs, top 100 cerebellar iLIs, and top 250 cerebrocerebellar iLIs. To derive a single metric for each specific network, iLI values involved in these left- and right-lateralized regions were then averaged for each individual.

Semantic decision task. Fifty-five subjects each performed three task-based fMRI runs of an abstract/concrete semantic classification task (Demb et al. 1995; Desmond et al. 1995). Our design manipulated familiarity to isolate regions specifically involved in controlled semantic retrieval. During the prescan familiarization phase, subjects repeatedly classified the same four words (2 abstract words and 2 concrete words) for five repetitions. During the scan, each run consisted of four 30-s “novel” blocks of task, four 30-s “familiar” blocks, and four 30-s block of fixation. In each novel block, 10 novel words (5 concrete words and 5 abstract words in random order) were presented for 2 s with a 1-s interstimulus interval. In the familiar block, the four practiced words were presented repeatedly. The subject's task was to indicate if each word was concrete or abstract independent of novelty. In total, 120 novel words and 4 familiar words were used. Participants were instructed to respond by pressing a single key with the index finger of each hand. The MRI data acquisition parameters were identical to the resting-state scan described above except that 124 time points were acquired in each task run. Data were first analyzed using the general linear model in the participants' native fMRI space. Brain regions participating in controlled semantic retrieval were isolated by contrasting the novel versus familiar condition. Maps of individual participants including the cerebrum and cerebellum were transformed into the FreeSurfer nonlinear volumetric space for group analysis.

Visualization. While all analyses were performed in FreeSurfer surface and volumetric space, for the purpose of visualization, maps were displayed in the volume space using the Montreal Neurological Institute atlas space and for the surface on the left and right inflated population-average, landmark- and surface-based cortical surfaces using Caret software (Van Essen 2005). Cerebellar nomenclature uses the conventions of Larsell (1970) as described in the MRI atlas of Schmahmann et al. (1999, 2000). Diedrichsen et al. (2009) was also relied on to determine fissure and lobule locations.

RESULTS

The cerebellum is lateralized in function. We first identified functionally lateralized regions of the cerebellum. An iLI was constructed for regions throughout the cerebellum based on spontaneous functional activity by examining relative correlation strengths between seed and target regions in the two cerebellar hemispheres, similar to the approach described in our previous study of the cerebral cortex (Liu et al. 2009). One thousand healthy young subjects were divided into discovery ($n = 500$) and replication ($n = 500$) samples. Cubic regions ($n = 275$, $8 \times 8 \times 8$ mm) were defined in the left cerebellar hemisphere, and each region was then registered to the right hemisphere using a nonlinear transformation (Andersson et al. 2007). For each pair of regions within the left hemisphere, the homologous pair of regions in the right hemisphere was identified, resulting in 37,675 possible region pairs in each cerebellar hemisphere. A cerebellar iLI was computed based on the asymmetry of the functional correlation strengths between the two homologous region pairs (see MATERIALS AND METHODS). These 37,675 laterality indices were averaged across the subjects and then ranked to find those cerebellar regions with the strongest asymmetries.

The cerebellar regions involved in the 100 most strongly lateralized pairs were identified in the discovery sample (Fig. 2, *left*). The broad patterns of asymmetry were reproduced in the replication sample (Fig. 2, *right*). Although we chose the top 100 lateralized pairs, we tested other selection thresholds and found the maps derived from 150, 200, and 250 lateralized pairs to be qualitatively similar.

To obtain the most stable map of the lateralized regions in the human cerebellum, the same analysis was performed in the full sample of 1,000 subjects (Fig. 3). The results revealed prominent functional specialization in the cerebellum. The most right-lateralized cerebellar regions were localized mainly in crus I and II and the posterior part of lobule VI. The most left-lateralized regions were localized mainly in lobules VI and VIII and the anterior portion of crus I/II.

Functional lateralization emerges in large-scale cerebro-cerebellar networks. Previous clinical and imaging studies have indicated that cerebellar asymmetry may covary with cerebral asymmetry. Here, we examined the relation between cerebellar and cerebral asymmetry. Spontaneous functional activity in the cerebral cortex was projected to the surface of a symmetric brain template (see MATERIALS AND METHODS). The surface of each cerebral hemisphere was tessellated into 642 triangular vertices, resulting in 205,761 possible region pairs. Connectivity strength between each cerebral region pair was compared with the homologous region pair to determine the cerebral iLI. The 100 most lateralized region pairs were identified in the full sample of 1,000 subjects (Fig. 4C). The left-lateralized regions involved the inferior frontal gyrus,

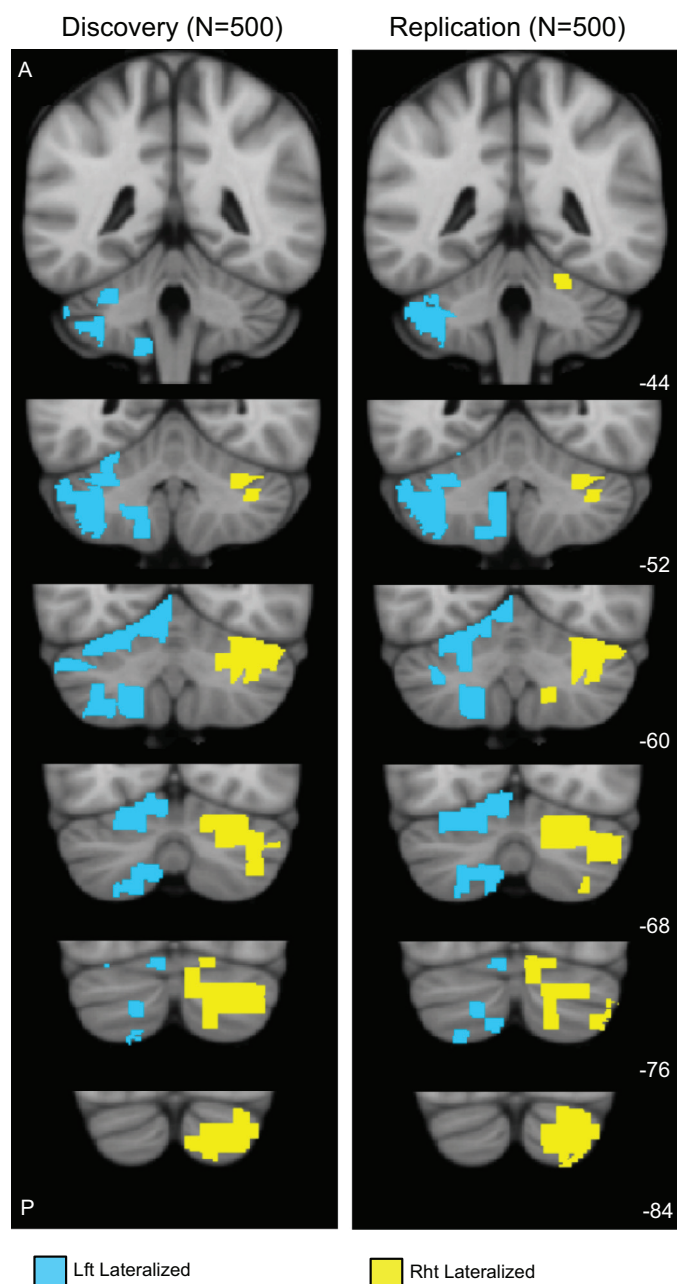


Fig. 2. Cerebellar asymmetry for the discovery ($n = 500$) and replication ($n = 500$) samples. Functional asymmetry was computed using intrinsic connectivity by examining relative correlation strengths between seed and target regions in the two cerebellar hemispheres; 275 regions were defined in each hemisphere of the cerebellum, resulting in 37,675 possible pairs within each hemisphere (see MATERIALS AND METHODS). The regions involved in the 100 most strongly lateralized pairs are shown in blue (left lateralized) and yellow (right lateralized). Left-lateralized regions are shown in the left cerebellum. The patterns of asymmetry largely replicated between the discovery and replication samples. The coordinates at the bottom right represent the section level (in mm) in the Montreal Neurological Institute atlas space.

superior temporal gyrus, and temporal pole (Fig. 4C, *right*). The 100 most right-lateralized pairs involved the insula and angular gyrus (Fig. 4C, *left*). These lateralized cerebral regions replicate several of the networks previously found using a volume-based approach with a smaller data set (Liu et al. 2009). However, certain aspects of the prior results were mitigated by the use of the symmetric surface registered

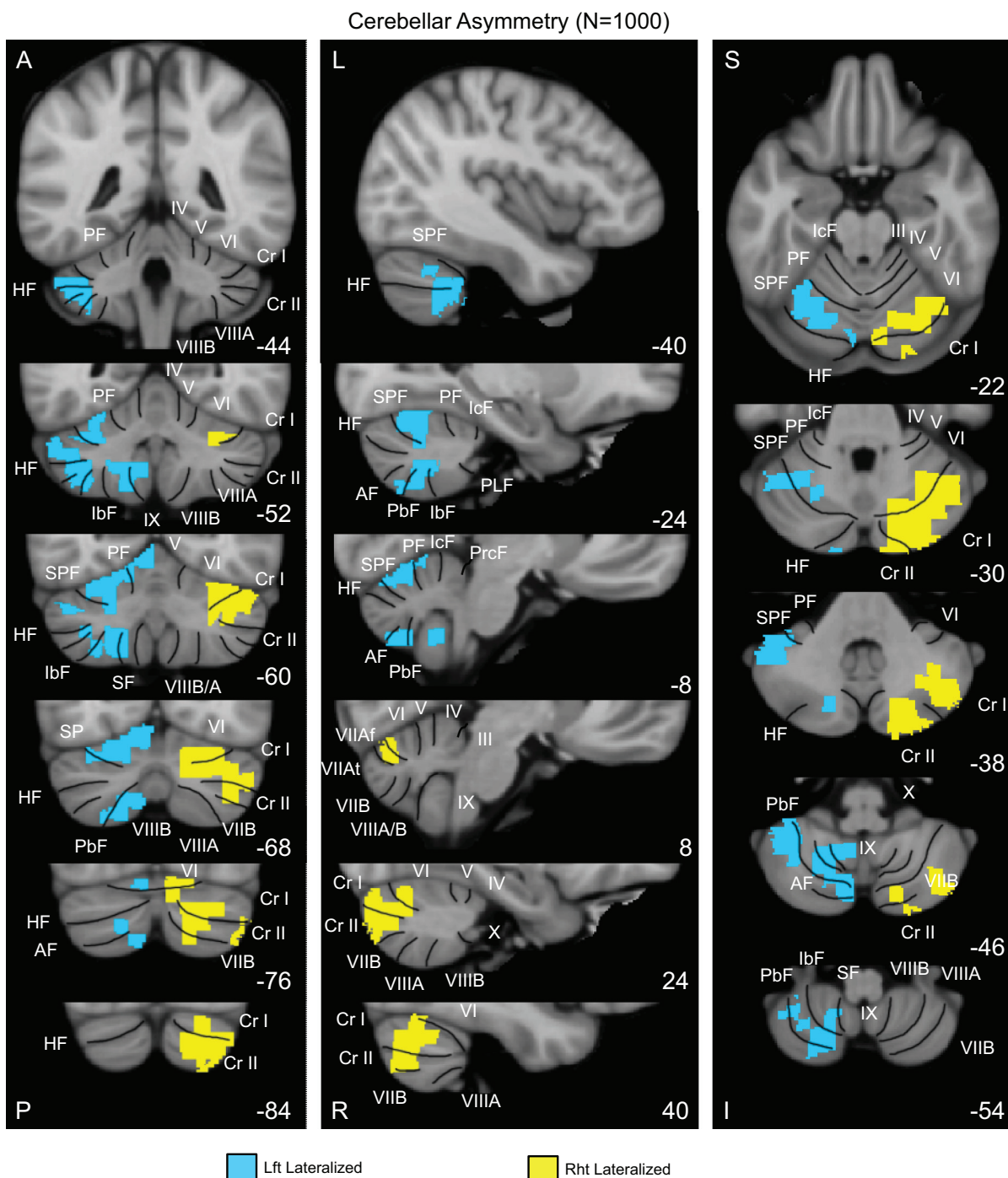


Fig. 3. A map of human cerebellar asymmetry based on functional connectivity in the full sample of 1,000 individuals. The most left-lateralized regions (shown in blue) were localized mainly in lobules VI and VIII and the most anterior part of crus I/II. The most right-lateralized cerebellar regions (shown in yellow) were localized mainly in crus I and II and lobule VI. Coronal (right), sagittal (middle), and transverse (left) images are shown. Major fissures are shown on the left, and lobules are shown on the right based on the studies of Schmahmann et al. (1999, 2000). PF, primary fissure; SPF, superior posterior fissure; HF, horizontal fissure; AF, ansoparamedian fissure; PbF, prepyramidal/prebiventer fissure; IbF, intrabiventer fissure; SF, secondary fissure; IcF, intraculminate fissure; PLF, posterolateral fissure; PrcF, preculminate fissure; A, anterior; P, posterior; L, left; R, right; S, superior; I, inferior. The coordinates at the bottom right represent the section level in the MNI atlas space.

template, suggesting some components in the prior analyses were due to asymmetries in anatomy that are better accounted for by the present approach.

Cerebrocerebellar coupling was next examined to explore if the functional connectivity between the cerebral cortex and contralateral cerebellum demonstrates asymmetry. The

642 regions in the left cerebral hemisphere were paired with the 275 regions in the right cerebellum, resulting in 176,550 possible cerebrocerebellar region pairs. Their mirroring region pairs were identified in the right cerebral cortex and left cerebellum. The cerebrocerebellar iLI was computed by comparing the correlation strengths of the two mirroring

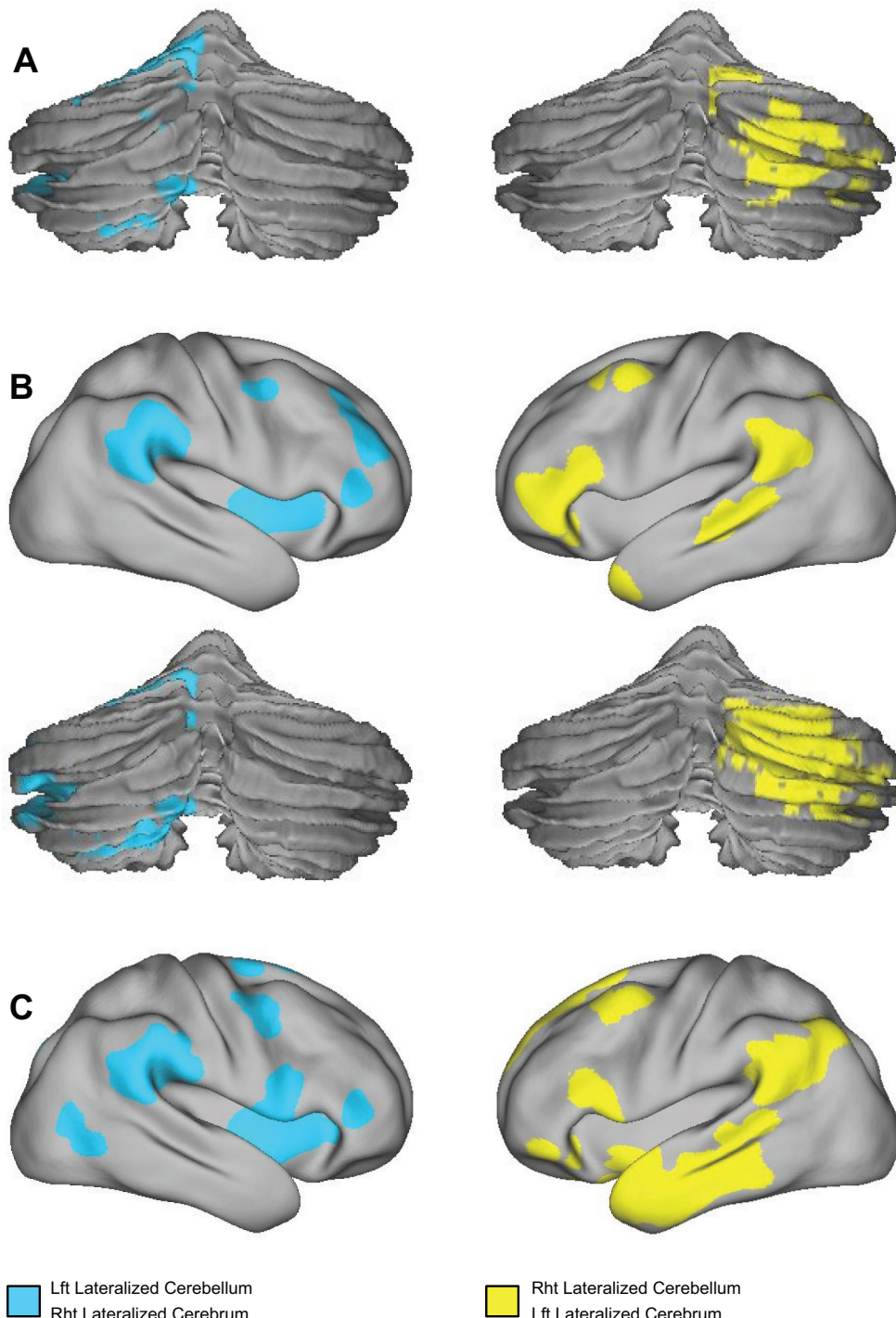


Fig. 4. Cerebral and cerebrocerebellar asymmetry. *A*: cerebellar asymmetry was plotted for the 100 most lateralized seed region pairs within the cerebellum. Cerebellar asymmetry maps were derived from the results shown in Fig. 2, estimated independently of cerebral asymmetry, and shown here on the surface to allow comparison with the maps of asymmetry based on cerebrocerebellar connectivity. *B*: cerebrocerebellar asymmetry was plotted with the 250 most lateralized seed region pairs visualized on the surface where each pair involves a region in the cerebral cortex and a region in the contralateral cerebellum. *C*: cerebral asymmetry was plotted with the 100 most lateralized seed region pairs for the cerebral cortex displayed on the surface. Cerebral asymmetry was estimated independently of cerebellar asymmetry. Cortical surface projections are shown using the population-average, landmark- and surface-based atlas (Van Essen 2005).

region pairs. The 250 cerebrocerebellar region pairs most lateralized in the left cerebrum/right cerebellum involved the inferior frontal gyrus, superior temporal gyrus, and temporal pole in the cerebral cortex, along with crus I/II in the cerebellum (Fig. 4*B, right*). The 250 region pairs most lateralized in right cerebrum/left cerebellum included the angular gyrus, parietal operculum, and insula in the cerebral cortex along with lobules VI and VIII in the cerebellum (Fig. 4*B, left*). The cerebral and cerebellar regions involved in these lateralized cerebrocerebellar couplings (Fig. 4*B*) largely overlapped with regions identified using cerebral

connectivity alone (Fig. 4*C*) and using cerebellar connectivity alone (Fig. 4*A*).

The laterality analyses described above all suggest that nonmotor regions of the cerebellum are functionally asymmetric (Fig. 4). Here, we examined whether these lateralized regions in the cerebellum and cerebral cortex belong to the same functional networks. We based these analyses on our prior parcellation of the cerebrum (Yeo et al. 2011) and cerebellum (Buckner et al. 2011) into seven functional networks. In that earlier analysis, each voxel in the cerebellum was labeled as a member of a particular network if it has

maximal functional correlation with the cerebral network. Projection of the present cerebral and cerebellar asymmetries onto the network parcellations revealed that the lateralized cerebral and cerebellar regions (Fig. 5, A and B) belonged to two specific association networks (Fig. 5C). Note that the cerebellar and cerebral asymmetry maps were computed independently and were affected differently by acquisition asymmetries (e.g., asymmetries in the MRI field) and anatomic asymmetries. Thus, the convergence of functional asymmetries on the same networks within the cerebrum and cerebellum is not obligated and suggests parallel functional organization.

Cerebellar lateralization parallels cerebral lateralization across individuals. We turned to individual differences to explore further the possibility that cerebellar lateralization tracks cerebral lateralization. For this analysis, the lateralized regions identified in the discovery sample were examined in the individual subjects within the replication sample. The most lateralized cerebral and cerebellar regions pairs were first determined in the discovery sample (same process as shown in Fig. 4). For each individual in the replication sample, cerebral and cerebellar laterality indices were then computed by averaging the iLI of these lateralized pairs within each hemisphere. Therefore, 4 iLIs were derived for each of the 500 subjects, corresponding to the left-lateralized and right-lateralized regions determined by the cerebral and cerebellar couplings, respectively. The distributions of these iLIs in the replication

sample showed strong lateralization (Fig. 6), suggesting that most individuals have lateralized cerebral and cerebellar functions.

We next tested whether cerebellar lateralization is associated with cerebral lateralization across subjects. For this analysis, we used the full sample. The cerebral iLI and cerebellar iLI were significantly correlated for both the left cerebellum/right cerebrum and the right cerebellum/left cerebrum (both $P < 0.001$; Fig. 7). Again, because the cerebral and cerebellar values were independently computed, this was not an obligated result. Rather, the relation indicates that significant between-subject variance in cerebral asymmetry is matched by cerebellar asymmetry.

Cerebellar asymmetry at rest predicts cerebral asymmetry during semantic classification. An implication of the above results is that functional asymmetry estimates of the cerebellum capture stable properties of functional organization within an individual. However, it is difficult to rule out other potential contributing sources of variance (such as momentary functional shifts in organization) because only a single type of measure was made at the same time for both the cerebellum and cerebrum. Here, we asked whether functional asymmetry measured in the cerebellum at rest is associated with task-based functional asymmetry measurements.

At the group level, strong lateralization was seen in the lateral prefrontal cortex and crus I/II in the cerebellum for

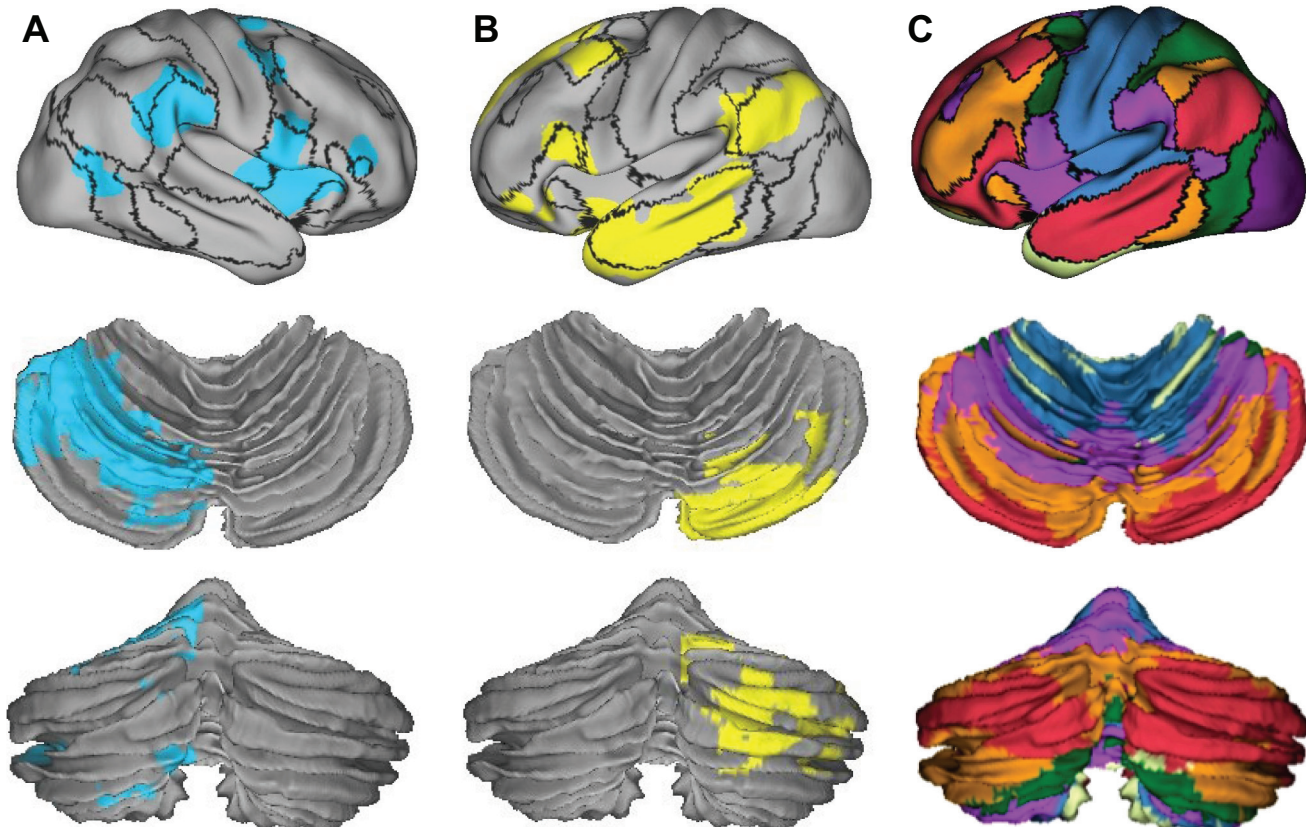


Fig. 5. Lateralized regions in the cerebral cortex and cerebellum belong to the same functional networks. Lateralized cerebral and cerebellar regions (A and B) were plotted on the surface with boundaries of functional connectivity networks from Yeo et al. (2011) illustrated with black lines. A: right-lateralized cerebral/left-lateralized cerebellar regions. B: left-lateralized cerebral/right-lateralized cerebellar regions. C: cerebellar segmentation based on coupling to cerebral networks according to Buckner et al. (2011). Each color in the cerebellar segmentation indicates which cerebral network showed the greatest coupling. What can be gleaned from these comparisons is that the most asymmetric regions of the cerebellum correspond to the salience ventral attention network (purple in C) and the default network (red in C). The networks displaying the strongest asymmetry in the cerebral cortex corresponded to their coupled networks in the cerebellum, which also displayed the greatest degree of asymmetry.

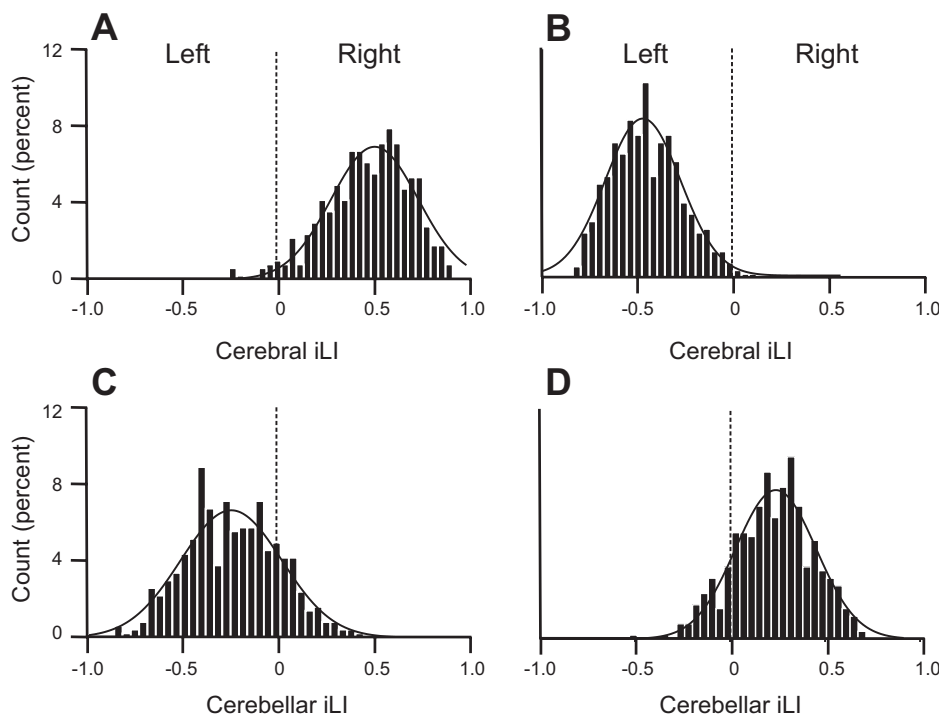


Fig. 6. Quantitative estimates of asymmetry for individuals. Lateralized regions were defined in the discovery sample ($n = 500$) independently for the cerebrum and cerebellum. Laterality indices from each individual from the replication sample were then computed as the mean laterality index separately for the left- and right-lateralized regions. The resulting cerebral and cerebellar iLIs are shown in A–D for the replication sample of 500 subjects. iLIs were plotted for the lateralized regions identified by cerebral connectivity (A and B) and cerebellar connectivity (C and D). iLIs for right-lateralized cerebral/left-lateralized cerebellar regions (yellow regions in Fig. 3) are shown in A and C. iLIs for left-lateralized cerebral/right-lateralized cerebellar regions (blue regions in Fig. 3) are shown in B and D. A positive iLI value reflects right dominance. Curves represent the Gaussian fit. Note that the distributions were strongly lateralized but reversed for the cerebrum and cerebellum.

novel as contrast to familiar semantic classification (Fig. 8A). These activated cerebral and cerebellar regions overlapped with the lateralized regions identified by intrinsic connectivity (see Fig. 4, A and B). We next computed the language laterality index for the individual subjects using an approach previously described in Liu et al. (2009). The language laterality index was computed independently for the cerebral cortex and cerebellum (Fig. 8B). Cerebral and cerebellar laterality indices during the task exhibited a strong correlation ($r = -0.91$, $P < 0.001$), suggesting that language lateralization in the cerebellum mirrors language lateralization in the contralateral cerebrum. We then estimated the cerebellar iLI of each individual using the right-lateralized cerebellar region (Fig. 8C). A moderate correlation ($r = -0.51$, $P < 0.001$) was observed between the right cerebellar iLI and the task-based language laterality index in the cerebral cortex. These results further support that cerebellar asymmetry is associated with cerebral asymmetry.

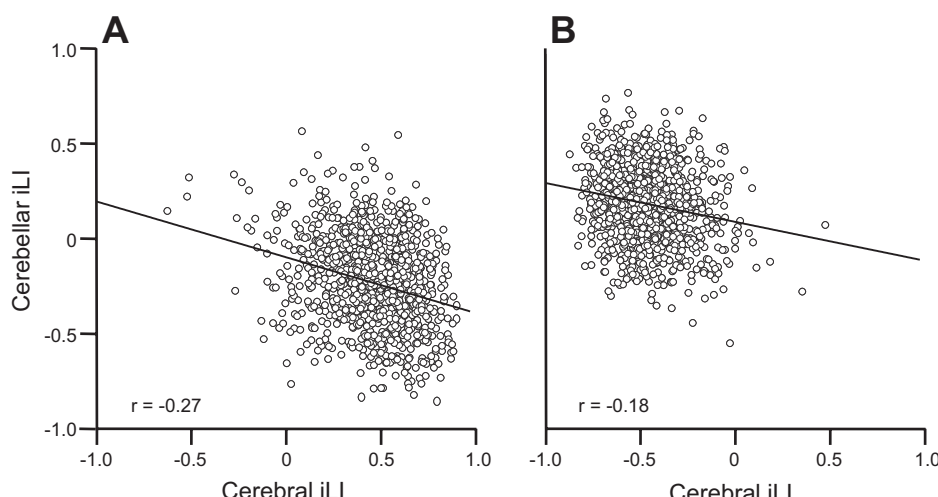


Fig. 7. Quantitative estimates of cerebral asymmetry track cerebellar asymmetry. The relation between cerebral iLI and cerebellar iLI, which were derived independently from one another for each subject, was plotted for all 1,000 subjects. A: iLIs from the right-lateralized cerebral/left-lateralized cerebellar regions. B: iLIs from the left-lateralized cerebral/right-lateralized cerebellar regions. The relations were both significant ($P < .001$), indicating that the degree of functional asymmetry for the cerebral cortex for an individual is associated with the degree of asymmetry for the cerebellum.

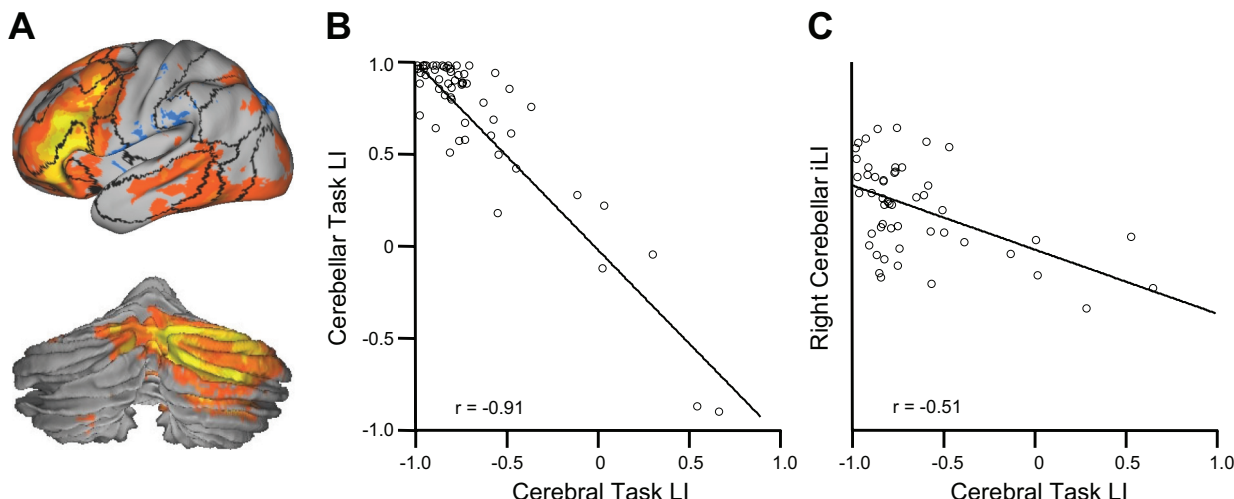


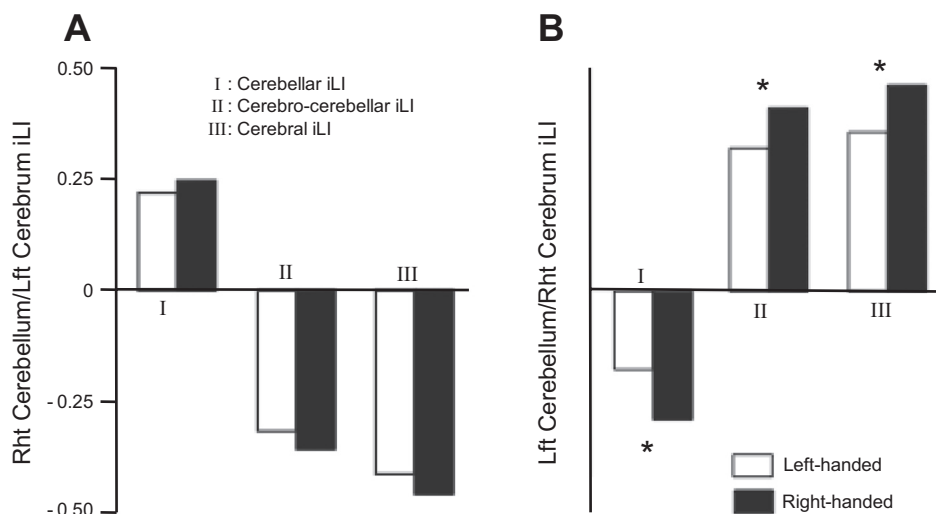
Fig. 8. Cerebellar lateralization predicts cerebral lateralization during a language task. *A*: 55 young healthy subjects participated in a semantic decision task. Regions activated by the task were strongly lateralized in both the cerebral cortex and cerebellum. *B*: task-based language lateralization in the cerebellum predicted language lateralization in the cerebral cortex ($r = -0.91$, $P < 0.001$). *C*: intrinsic lateralization estimated based on the right-lateralized cerebellar regions predicted task-based language lateralization in the cerebral cortex ($r = -0.51$, $P < 0.001$). LI, laterality index.

The cerebellar regions with the highest levels of asymmetry, defined as coupling patterns that are stronger in one cerebellar hemisphere than the other, are all linked to the cerebral association cortex. We have previously parcellated the human brain into cerebral networks (Yeo et al. 2011) and their corresponding cerebellar networks (Buckner et al. 2011). Using these parcellations as a reference, we further observed that the most lateralized regions in the cerebellum fall within two networks that are also those most strongly lateralized in the cerebrum. When functional asymmetries were computed at the level of individual subjects, the degree of asymmetry of the cerebellum correlated with asymmetry of the cerebrum, and left-handed individuals demonstrated reduced asymmetry in the cerebellum paralleling effects in the cerebrum. These findings all suggest that lateralization emerges as a unitary property of large-scale circuits that connect the cerebral cortex and cerebellum. Those networks that are strongly lateralized within the cerebrum are also strongly lateralized within the cerebellum; those individuals with the most functionally asymmetric cerebrums also possess the most asymmetric cerebellums.

The cerebellum is functionally asymmetric for regions linked to association but not the motor cortex. Cerebellar regions associated with motor function display minimal functional asymmetries. This observation may seem counterintuitive given the established crossed laterality of cerebrocerebellar circuits: the cerebral hemispheres project primarily to the contralateral cerebellar hemispheres. To understand this paradoxical observation, it is important to distinguish the preferential contralateral organization of cerebrocerebellar circuits from asymmetric functional organization.

Results from analysis of functional connectivity in the human are fully consistent with anatomic crossed laterality. For example, both Krienen and Buckner (2009) and O'Reilly et al. (2010) reported that cerebral regions within the left and right motor cortex display strong preferential correlations with the contralateral cerebellum. Lu et al. (2011) recently showed that focal pontine infarcts associated with lateralized hemiparesis disrupt coupling between the motor cortex and the contralateral cerebellum. If anything, regional variability in functional connectivity analyses has tended to favor motor regions displaying

Fig. 9. Functional asymmetry is associated with handedness. *A*: cerebellar, cerebrocerebellar, and cerebral asymmetries estimated based on the yellow regions shown in Fig. 4 (left-lateralized cerebrum and right-lateralized cerebellum) displayed stronger asymmetry in right-handed individuals, but the handedness effect was not significant. *B*: the blue regions shown in Fig. 4 (right-lateralized cerebrum and left-lateralized cerebellum) exhibited a significant effect of handedness (* $P < 0.05$ in all three measures), with right-handed individuals showing stronger asymmetry than left-handed individuals.



the strongest preferential coupling patterns to the contralateral cerebellum in contrast to the ipsilateral cerebellum (e.g., see Fig. 5 in Krienen and Buckner 2009). Functional symmetry arises for motor regions of the cerebellum because the strengths of the contralateral coupling patterns for the left and right motor regions tend to be symmetric. That is, the strength of coupling from the left motor cortex to the right cerebellum is roughly the same strength as the strength of coupling from the right motor cortex to the left cerebellum.

In contrast, functional coupling for cerebellar regions linked to the association cortex show marked left-right asymmetries. Using intrinsic connectivity, Habas et al. (2009) first illustrated that frontoparietal networks linked to executive control are asymmetric, including major parts of crus I/II. The most asymmetric cerebrocerebellar circuits detected here involving the association cortex are shown in Figs. 3–5. For these regions, correlations between regions within one hemisphere are stronger than the homologous pairings for the opposite hemisphere, perhaps to be considered a form of dominance. Functional asymmetry of the cerebellum has previously been observed in task-based studies beginning with the seminal observations of Petersen et al. (1989). In a recent meta-analysis involving over 200 imaging studies (Stoodley and Schmahmann 2009), it was shown that the activation peaks for language tasks were lateralized to right lobule VI, crus I/Crus II, and midline lobule VIIA. In contrast, spatial processing showed greater left hemisphere activation, predominantly in lobule VI. Similar lateralization patterns were found in clinical populations. Language impairment can arise after right cerebellar hemisphere lesions, whereas visual-spatial difficulties may follow left cerebellar hemisphere damage (Fiez et al. 1992; Gottwald et al. 2004; Gross-Tsur et al. 2006; Hokkanen et al. 2006; Leggio et al. 2008; Riva and Giorgi 2000; Scott et al. 2001). Consistent with these imaging and clinical findings, our results indicate a right-lateralized cerebellar network that includes crus I/II and a portion of lobule VI, which couples to a left-lateralized cerebral network involving the inferior frontal gyrus, superior temporal gyrus, and temporal pole in the cerebral cortex. These regions include (but also extend beyond) traditional language regions in the cerebral cortex and the cerebellar regions commonly activated by language-related tasks. A left-lateralized cerebellar network included lobules VI and VIII, which couples to a right-lateralized cerebral network involving the insula, parietal operculum, and angular gyrus.

Cerebellar lobules VI and VIII are sometimes considered as motor/sensory regions. However, their role in cognitive functions was also widely recognized, especially in functional imaging studies (e.g., Stoodley et al. 2009 and Kirschen et al. 2005). In the present study, we observed lobules VI/VIIIA aligned with an asymmetric network connecting to the angular gyrus, parietal operculum, and insula. Functional connectivity between lobule VI/VIIIA and cerebral regions implicated in cognitive function has also been observed in our previous work (Buckner et al. 2011). For example, when a seed region was placed in left cerebellar lobule VI, strong correlation was found in the right angular gyrus, parietal operculum, and insula. However, the connection between right lobule VI and the left cerebral cortex was weaker, presaging the asymmetries we focused on here. It is difficult to interpret the function of these asymmetric networks, and there have been many prior reports on their cerebral components (e.g., Habas et al. 2009; Yeo et al.

2011; Powers et al. 2011). What we are able to determine here is that the functional asymmetries present in the cerebral cortex are paralleled by asymmetries in the cerebellum.

Functional specialization may emerge simultaneously in the cerebral cortex and cerebellum. An important implication of our results is that lateralization may emerge in the form of large-scale cerebrocerebellar networks, causing a parallel specialization pattern in the cerebral cortex and cerebellum. Compared with the cerebral cortex, the cytoarchitecture in the cerebellum is much simpler. The same circuit is repeated throughout the cerebellar cortex (Ito 1984). Consequently, the functional specialization in the cerebellum does not likely arise from cytoarchitecture differences within the cerebellum but likely reflects the specialization of the multiple closed-loop circuits that connect the cerebellum to the cerebral cortex and other structures. This possibility is supported by clinical observations where patients shift cerebellar laterality after lesions in the cerebral cortex (Connor et al. 2006; Lidzba et al. 2008).

If cerebellar asymmetry reflects the specialization of the large-scale cerebrocerebellar circuits, then cerebral asymmetry may be reliably estimated in the cerebellum. Assessing functional lateralization in individual subjects is often hampered by anatomic asymmetries in the cerebral cortex. Cerebral anatomic asymmetries exist in almost all scales from the microscopic cytoarchitecture to the macroscopic folding patterns and surface areas. Therefore, quantification of the functional asymmetry is often confounded by anatomic factors, sometimes in mundane ways, such as how a technique differentially samples the anatomy on the left and right side of the brain (e.g., corresponding fMRI voxels in the left and right hemispheres). For example, in our previous study, we observed a strong lateralization in the primary visual area (Liu et al. 2009). This lateralization diminished in the present study, where we used a symmetric brain template and applied a surface-based alignment that better accounts for anatomic asymmetry. However, even with the symmetric template, misalignment could still cause erroneous results. Functional asymmetry estimated in the cerebellum is less affected by anatomic asymmetry (or at the very least, affected differently). We found that the degree of lateralization in the cerebellum correlated with the lateralization in the cerebrum, suggesting the force driving cerebral lateralization may similarly cause the cerebellar lateralization but in the contralateral hemisphere. These findings suggest the possibility of investigating cerebral functional asymmetry by way of the cerebellum, which is less confounded by anatomic factors.

Some cerebellar regions may appear in both left-lateralized and right-lateralized connections. It should be noted that these regions do not always couple to homotopic regions in the cerebral cortex, at least to the same degree. For example, functional connectivity between left lobule VI and the right insular cortex is stronger than the homotopic connectivity pattern. Functional connectivity between right lobule VI and the left dorsal prefrontal cortex also appears to be stronger than the homotopic regions. Therefore, lobule VI is included in both left-lateralized and right-lateralized coupling patterns, but these differential connectivity patterns involve distinct cerebral regions.

An interesting observation is that cerebellar asymmetry appears to be weaker than cerebral asymmetry. A possible explanation of this difference is that the asymmetries are

primarily driven by the cerebral cortex and cerebellum simply echoes these specializations indirectly by way of its anatomic connectivity. It is also possible the differential asymmetry between the cerebrum and cerebellum is an artifact of technical limitations. It is more difficult to estimate cerebellar properties owing to the small size of the structure and its fine cortical folding pattern.

Conclusions. The present results are most consistent with the possibility that the cerebellum possesses a roughly homotopic map of the cerebral cortex including the prominent asymmetries of the association cortex. Functional asymmetry likely emerges simultaneously in the cerebrum and cerebellum as the large-scale cerebrocerebellar circuits become specialized during development. Asymmetries are particularly prominent in cerebellar regions linked to the association cortex, consistent with the marked functional asymmetries that have been long observed in these systems in the cerebral cortex.

ACKNOWLEDGMENTS

The authors thank Mert R. Sabuncu and Douglas Greve for providing the symmetric brain template as well as Rebecca Shafee, Jorge Sepulcre, B. T. Thomas Yeo, Avram Holmes, Sophia Mueller, and Fenna Krienen for thoughtful discussions and technical assistance.

Data for this project come from the Brain Genomics Superstruct Project.

GRANTS

This work was supported by National Institutes of Health Grants K25-NS-069805, AG-021910, and P41-RR-14074, a National Alliance for Research on Schizophrenia and Depression Young Investigator grant, Massachusetts General Hospital-University of California-Los Angeles Human Connectome Project U54MH091665, the Simons Foundation, and the Howard Hughes Medical Institute.

DISCLOSURES

No conflicts of interest, financial or otherwise, are declared by the author(s).

AUTHOR CONTRIBUTIONS

Author contributions: D.W. and H.L. conception and design of research; D.W. and H.L. performed experiments; D.W. and H.L. analyzed data; D.W., R.L.B., and H.L. interpreted results of experiments; D.W. and R.L.B. prepared figures; D.W. drafted manuscript; D.W., R.L.B., and H.L. approved final version of manuscript; R.L.B. and H.L. edited and revised manuscript.

REFERENCES

- Amunts K, Schleicher A, Burgel U, Mohlberg H, Uylings HB, Zilles K. Broca's region revisited: cytoarchitecture and intersubject variability. *J Comp Neurol* 412: 319–341, 1999.
- Amunts K, Schleicher A, Ditterich A, Zilles K. Broca's region: cytoarchitectonic asymmetry and developmental changes. *J Comp Neurol* 465: 72–89, 2003.
- Anderson JS, Druzgal TJ, Froehlich A, DuBray MB, Lange N, Alexander AL, Abildskov T, Nielsen JA, Cariello AN, Cooperrider JR, Bigler ED, Lainhart JE. Decreased interhemispheric functional connectivity in autism. *Cereb Cortex* 21: 1134–1146, 2011.
- Andersson JLR, Jenkinson M, Smith S. *Non-Linear Registration, aka Spatial Normalisation. Technical Report TR07JA2*. Oxford: Oxford Centre for Functional MRI of the Brain, 2007.
- Biswal B, Yetkin FZ, Haughton VM, Hyde JS. Functional connectivity in the motor cortex of resting human brain using echo-planar MRI. *Magn Reson Med* 34: 537–541, 1995.
- Buckner RL, Krienen FM, Castellanos A, Diaz JC, Yeo BT. The organization of the human cerebellum estimated by intrinsic functional connectivity. *J Neurophysiol* 106: 2322–2345, 2011.
- Choi EY, Yeo BT, Buckner RL. The organization of the human striatum estimated by intrinsic functional connectivity. *J Neurophysiol* 108: 2242–2263, 2012.
- Clower DM, West RA, Lynch JC, Strick PL. The inferior parietal lobule is the target of output from the superior colliculus, hippocampus, and cerebellum. *J Neurosci* 21: 6283–6291, 2001.
- Connor LT, DeShazo Braby T, Snyder AZ, Lewis C, Blasi V, Corbetta M. Cerebellar activity switches hemispheres with cerebral recovery in aphasia. *Neuropsychologia* 44: 171–177, 2006.
- Dale AM, Fischl B, Sereno MI. Cortical surface-based analysis. I. Segmentation and surface reconstruction. *Neuroimage* 9: 179–194, 1999.
- Demb JB, Desmond JE, Wagner AD, Vaidya CJ, Glover GH, Gabrieli JD. Semantic encoding and retrieval in the left inferior prefrontal cortex: a functional MRI study of task difficulty and process specificity. *J Neurosci* 15: 5870–5878, 1995.
- Desmond JE, Sum JM, Wagner AD, Demb JB, Shear PK, Glover GH, Gabrieli JD, Morrell MJ. Functional MRI measurement of language lateralization in Wada-tested patients. *Brain* 118: 1411–1419, 1995.
- Diedrichsen J, Balsters JH, Flavell J, Cussans E, Ramnani N. A probabilistic MR atlas of the human cerebellum. *Neuroimage* 46: 39–46, 2009.
- Evarts EV, Thach WT. Motor mechanisms of the CNS: cerebrocerebellar interrelations. *Annu Rev Physiol* 31: 451–498, 1969.
- Fiez JA, Petersen SE, Cheney MK, Raichle ME. Impaired non-motor learning and error detection associated with cerebellar damage. A single case study. *Brain* 115: 155–178, 1992.
- Fischl B, Liu A, Dale AM. Automated manifold surgery: constructing geometrically accurate and topologically correct models of the human cerebral cortex. *IEEE Trans Med Imaging* 20: 70–80, 2001.
- Fischl B, Salat DH, Busa E, Albert M, Dieterich M, Haselgrove C, van der Kouwe A, Killiany R, Kennedy D, Klaveness S, Montillo A, Makris N, Rosen B, Dale AM. Whole brain segmentation: automated labeling of neuroanatomical structures in the human brain. *Neuron* 33: 341–355, 2002.
- Fischl B, Salat DH, van der Kouwe AJ, Makris N, Segonne F, Quinn BT, Dale AM. Sequence-independent segmentation of magnetic resonance images. *Neuroimage* 23, Suppl 1: S69–S84, 2004a.
- Fischl B, Sereno MI, Dale AM. Cortical surface-based analysis. II: Inflation, flattening, and a surface-based coordinate system. *Neuroimage* 9: 195–207, 1999a.
- Fischl B, Sereno MI, Tootell RB, Dale AM. High-resolution intersubject averaging and a coordinate system for the cortical surface. *Hum Brain Mapp* 8: 272–284, 1999b.
- Fischl B, van der Kouwe A, Destrieux C, Halgren E, Segonne F, Salat DH, Busa E, Seidman LJ, Goldstein J, Kennedy D, Caviness V, Makris N, Rosen B, Dale AM. Automatically parcellating the human cerebral cortex. *Cereb Cortex* 14: 11–22, 2004b.
- Fox MD, Snyder AZ, Vincent JL, Corbetta M, Van Essen DC, Raichle ME. The human brain is intrinsically organized into dynamic, anticorrelated functional networks. *Proc Natl Acad Sci USA* 102: 9673–9678, 2005.
- Galuske RA, Schlotte W, Bratzke H, Singer W. Interhemispheric asymmetries of the modular structure in human temporal cortex. *Science* 289: 1946–1949, 2000.
- Gazzaniga MS. Cerebral specialization and interhemispheric communication: does the corpus callosum enable the human condition? *Brain* 123: 1293–1326, 2000.
- Geschwind N, Galaburda AM. Cerebral lateralization. Biological mechanisms, associations, and pathology: I. A hypothesis and a program for research. *Arch Neurol* 42: 428–459, 1985.
- Geschwind N, Levitsky W. Human brain: left-right asymmetries in temporal speech region. *Science* 161: 186–187, 1968.
- Gottwald B, Wilde B, Mihajlovic Z, Mehdorn HM. Evidence for distinct cognitive deficits after focal cerebellar lesions. *J Neurol Neurosurg Psychiatry* 75: 1524–1531, 2004.
- Greve DN, Fischl B. Accurate and robust brain image alignment using boundary-based registration. *Neuroimage* 48: 63–72, 2009.
- Gross-Tsur V, Ben-Bashat D, Shalev RS, Levav M, Sira LB. Evidence of a developmental cerebello-cerebral disorder. *Neuropsychologia* 44: 2569–2572, 2006.
- Habas C, Kamdar N, Nguyen D, Prater K, Beckmann CF, Menon V, Greicius MD. Distinct cerebellar contributions to intrinsic connectivity networks. *J Neurosci* 29: 8586–8594, 2009.
- Hill J, Dierker D, Neil J, Inder T, Knutson A, Harwell J, Coalson T, Van Essen D. A surface-based analysis of hemispheric asymmetries and folding of cerebral cortex in term-born human infants. *J Neurosci* 30: 2268–2276, 2010.

- Hokkanen LS, Kauranen V, Roine RO, Salonen O, Kotila M.** Subtle cognitive deficits after cerebellar infarcts. *Eur J Neurol* 13: 161–170, 2006.
- Ito M.** *The Cerebellum and Neural Control*. New York: Raven, 1984.
- Jenkinson M, Bannister P, Brady M, Smith S.** Improved optimization for the robust and accurate linear registration and motion correction of brain images. *Neuroimage* 17: 825–841, 2002.
- Kelly RM, Strick PL.** Cerebellar loops with motor cortex and prefrontal cortex of a nonhuman primate. *J Neurosci* 23: 8432–8444, 2003.
- Kemp JM, Powell TP.** The connexions of the striatum and globus pallidus: synthesis and speculation. *Philos Trans R Soc Lond B Biol Sci* 262: 441–457, 1971.
- Kirschen MP, Chen SH, Schraedley-Desmond P, John E, Desmond JE.** Load-and practice-dependent increases in cerebro-cerebellar activation in verbal working memory: an fMRI study. *Neuroimage* 24: 462–472, 2005.
- Krienen FM, Buckner RL.** Segregated fronto-cerebellar circuits revealed by intrinsic functional connectivity. *Cereb Cortex* 19: 2485–2497, 2009.
- Larsell O.** (editor). *The Comparative Anatomy and Histology of the Cerebellum From Monotremes Through Apes*. Minneapolis, MN: Univ. of Minnesota Press, 1970.
- Leggio MG, Tedesco AM, Chiricozzi FR, Clausi S, Orsini A, Molinari M.** Cognitive sequencing impairment in patients with focal or atrophic cerebellar damage. *Brain* 131: 1332–1343, 2008.
- Lidzba K, Wilke M, Staudt M, Krageloh-Mann I, Grodd W.** Reorganization of the cerebro-cerebellar network of language production in patients with congenital left-hemispheric brain lesions. *Brain Lang* 106: 204–210, 2008.
- Lu H, Shupplebeam SM, Sepulcre J, Hedden T, Buckner RL.** Evidence from intrinsic activity that asymmetry of the human brain is controlled by multiple factors. *Proc Natl Acad Sci USA* 106: 20499–20503, 2009.
- Lu J, Liu H, Zhang M, Wang D, Cao Y, Ma Q, Rong D, Wang X, Buckner RL, Li K.** Focal pontine lesions provide evidence that intrinsic functional connectivity reflects polysynaptic anatomical pathways. *J Neurosci* 31: 15065–15071, 2011.
- Luders E, Narr KL, Thompson PM, Rex DE, Jancke L, Toga AW.** Hemispheric asymmetries in cortical thickness. *Cereb Cortex* 16: 1232–1238, 2006.
- Milner B, Johnsrude I, Crane J.** Right medial temporal-lobe contribution to object-location memory. *Philos Trans R Soc Lond B Biol Sci* 352: 1469–1474, 1997.
- O'Reilly JX, Beckmann CF, Tomassini V, Ramnani N, Johansen-Berg H.** Distinct and overlapping functional zones in the cerebellum defined by resting state functional connectivity. *Cereb Cortex* 20: 953–965, 2010.
- Petersen SE, Fox PT, Posner MI, Mintun M, Raichle ME.** Positron emission tomographic studies of the processing of single words. *J Cogn Neurosci* 1: 153–170, 1989.
- Power JD, Cohen AL, Nelson SM, Wig GS, Barnes KA, Church JA, Vogel AC, Laumann TO, Miezin FM, Schlaggar BL, Petersen SE.** Functional network organization of the human brain. *Neuron* 72: 665–678.
- Riva D, Giorgi C.** The cerebellum contributes to higher functions during development: evidence from a series of children surgically treated for posterior fossa tumours. *Brain* 123: 1051–1061, 2000.
- Schmahmann JD, Doyon J, McDonald D, Holmes C, Lavoie K, Hurwitz AS, Kabani N, Toga A, Evans A, Petrides M.** Three-dimensional MRI atlas of the human cerebellum in proportional stereotaxic space. *Neuroimage* 10: 233–260, 1999.
- Schmahmann JD, Doyon J, Toga AW, Petrides M, Evans AC.** (editors). *MRI Atlas of the Human Cerebellum*. San Diego, CA: Academic, 2000.
- Schmahmann JD, Pandya DN.** The cerebrocerebellar system. *Int Rev Neurobiol* 41: 31–60, 1997.
- Scott RB, Stoodley CJ, Anslow P, Paul C, Stein JF, Sugden EM, Mitchell CD.** Lateralized cognitive deficits in children following cerebellar lesions. *Dev Med Child Neurol* 43: 685–691, 2001.
- Segonne F, Dale AM, Busa E, Glessner M, Salat D, Hahn HK, Fischl B.** A hybrid approach to the skull stripping problem in MRI. *Neuroimage* 22: 1060–1075, 2004.
- Segonne F, Pacheco J, Fischl B.** Geometrically accurate topology-correction of cortical surfaces using nonseparating loops. *IEEE Trans Med Imaging* 26: 518–529, 2007.
- Smith SM, Jenkinson M, Woolrich MW, Beckmann CF, Behrens TE, Johansen-Berg H, Bannister PR, De Luca M, Drobniak I, Flitney DE, Niazy RK, Saunders J, Vickers J, Zhang Y, De Stefano N, Brady JM, Matthews PM.** Advances in functional and structural MR image analysis and implementation as FSL. *Neuroimage* 23, Suppl 1: S208–S219, 2004.
- Snyder PJ, Bilder RM, Wu H, Bogerts B, Lieberman JA.** Cerebellar volume asymmetries are related to handedness: a quantitative MRI study. *Neuropsychologia* 33: 407–419, 1995.
- Stoodley CJ, Schmahmann JD.** Functional topography in the human cerebellum: a meta-analysis of neuroimaging studies. *Neuroimage* 44: 489–501, 2009.
- Strick PL.** How do the basal ganglia and cerebellum gain access to the cortical motor areas? *Behav Brain Res* 18: 107–123, 1985.
- Strick PL, Dum RP, Fiez JA.** Cerebellum and nonmotor function. *Annu Rev Neurosci* 32: 413–434, 2009.
- Toga AW, Thompson PM.** Mapping brain asymmetry. *Nat Rev Neurosci* 4: 37–48, 2003.
- van der Kouwe AJ, Benner T, Salat DH, Fischl B.** Brain morphometry with multiecho MPRAGE. *Neuroimage* 40: 559–569, 2008.
- Van Dijk KR, Hedden T, Venkataraman A, Evans KC, Lazar SW, Buckner RL.** Intrinsic functional connectivity as a tool for human connectomics: theory, properties, and optimization. *J Neurophysiol* 103: 297–321, 2010.
- Van Dijk KR, Sabuncu MR, Buckner RL.** The influence of head motion on intrinsic functional connectivity MRI. *Neuroimage* 59: 431–438.
- Van Essen DC.** A population-average, landmark- and surface-based (PALS) atlas of human cerebral cortex. *Neuroimage* 28: 635–662, 2005.
- Van Essen DC, Glasser MF, Dierker DL, Harwell J, Coalson T.** Parcellations and hemispheric asymmetries of human cerebral cortex analyzed on surface-based atlases. *Cereb Cortex* 22: 2241–2262, 2012.
- Vincent JL, Snyder AZ, Fox MD, Shannon BJ, Andrews JR, Raichle ME, Buckner RL.** Coherent spontaneous activity identifies a hippocampal-parietal memory network. *J Neurophysiol* 96: 3517–3531, 2006.
- White LE, Lucas G, Richards A, Purves D.** Cerebral asymmetry and handedness. *Nature* 368: 197–198, 1994.
- Witelson SF, Pallie W.** Left hemisphere specialization for language in the newborn. Neuroanatomical evidence of asymmetry. *Brain* 96: 641–646, 1973.
- Yeo BT, Krienen FM, Sepulcre J, Sabuncu MR, Lashkari D, Hollinshead M, Roffman JL, Smoller JW, Zollei L, Polimeni JR, Fischl B, Liu H, Buckner RL.** The organization of the human cerebral cortex estimated by intrinsic functional connectivity. *J Neurophysiol* 106: 1125–1165, 2011.